CRYSTAL GROWTH & DESIGN

Article

pubs.acs.org/crystal

Crystallization Optimization of Pharmaceutical Solid Forms with X-ray Compatible Microfluidic Platforms

Elizabeth M. Horstman,[†,⊥] Sachit Goyal,[†,⊥] Ashtamurthy Pawate,[†] Garam Lee,[†] Geoff G. Z. Zhang,[‡] Yuchuan Gong,*[,‡] and Paul J. A. Kenis*[,†]

[†]Department of Chemical & Biomolecular Engineering, University of Illinois at Urbana−Champaign, 600 South Mathews Avenue, Urbana, Illinois 61801, United States

[‡]Drug Product Development, Research and Development, AbbVie Inc., 1 North Waukegan Road, North Chicago, Illinois 60064, United States

Supporting Information

ABSTRACT: We describe a microfluidic approach to optimize crystallization of active pharmaceutical ingredients (APIs) and their solid forms (cocrystals) via crystal seeding. Subsequent on-chip X-ray diffraction is used to verify the crystal from. The microfluidic platform comprises an 8 × 9 well array that enables screening of seeding conditions (dilutions) by metering of API solution or API/cocrystal former solution and seed solution in ratios of 1:4 to 4:1, respectively, across each row. Slow solvent evaporation leads to seed growth and results in isolated diffraction quality crystals. To validate this microfluidic crystal seeding approach, three APIs (piroxicam, piracetam, and carbamazepine) and a cocrystal (carbamazepine/4-hydroxybenzoic acid) were used as model compounds. X-ray diffraction data was collected on-chip at room temperature to determine the crystal structure of the model compounds for comparison to published structural data. This on-chip seeding approach aided in crystallization of a desired solid form (e.g., a specific polymorph) over a mixture of solid forms. Easy handling, automated seeding and dilution, high throughput screening using small quantities of API (about 5 μg/well), and on-chip X-ray analysis of multiple crystals makes this platform attractive for solid form identification and characterization.

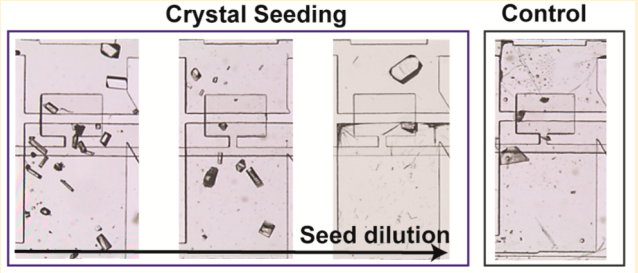

1. INTRODUCTION

The pharmaceutical industry devotes a significant amount of effort to identify a solid form of active pharmaceutical ingredients (API) with physicochemical properties suitable for product formulation. High-throughput screening approaches, often involving large robotic fluid handling systems, are used to obtain different solid forms of APIs such as polymorphs, cocrystals, or salts.[1−3] Analytical tools such as Raman spectroscopy, IR spectroscopy, powder X-ray diffraction, and single crystal X-ray diffraction are used to identify different solid forms. Single crystal X-ray diffraction is the most reliable way to solve the structure of pharmaceutical solid forms, because it easily distinguishes between different solid forms. The obtained crystal structure can also be used to simulate physical properties of the solid forms, reducing the need for extensive experimentation.[4]

To determine the crystal structure of APIs with X-ray diffraction, diffraction quality crystals need to be obtained. This can be challenging because a wide range of supersaturation levels need to be screened to obtain detailed phase behavior information, which can then guide crystallization of diffraction quality crystals.[5] Diffraction quality crystals can be grown by supersaturating a solution until it reaches the labile zone (nucleation zone) where nuclei form, then reduction of the supersaturation level of the solution to the metastable zone (crystal growth zone) will ensure growth of the nuclei into crystals, without additional nuclei being formed.[6,7] In principle, this sequence of steps can lead to monodisperse, diffraction quality crystals; however, precise control of supersaturation is not trivial.[8,9] Furthermore, the stochastic nature of the nucleation process often results in a broad crystal size distribution as well as poor control over the solid forms obtained.[10]

To overcome some of the aforementioned issues, advanced protocols to decouple crystal nucleation and growth have been developed, leading to more narrow crystal size distribution and better control over the specific solid form obtained.[11,12] For example, the seeding approach, in which previously formed microcrystals are used to initiate crystal growth (thus eliminating the stochastic nucleation process), can be used to grow large and monodisperse crystals.[6] During initial screening, pharmaceuticals and proteins tend to crystallize as microcrystals, spherulites, fine needles, or poorly formed crystals. These crystalline solids can be micronized and then used as

Received: October 31, 2014
Revised: January 5, 2015
Published: January 21, 2015

DOI: 10.1021/cg5016065
Cryst. Growth Des. 2015, 15, 1201−1209

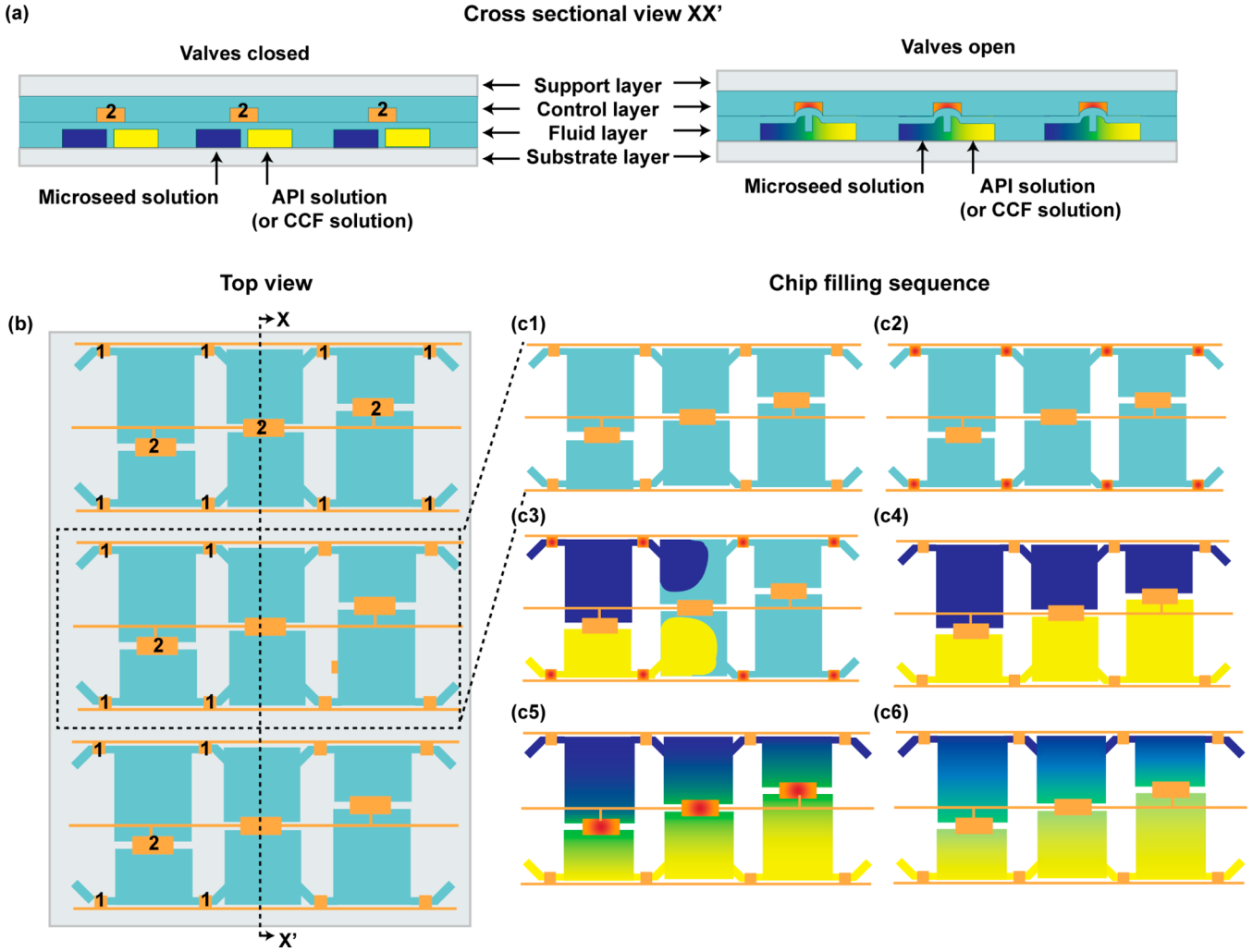

Figure 1. (a) Cross sectional view of three microfluidic crystallization wells showing the layered assembly of the platform. The platform is comprised of PDMS fluid and control layers sandwiched between layers of COC to minimize solvent loss and to provide rigidity. Diffusional mixing occurs between adjacent wells when the mixing valve (2) is actuated. (b) Top view of a 3 × 3 array of microfluidic crystallization wells representing the 8 × 9 array of microfluidic crystallization wells in the fabricated platform. The top view shows adjacent microseed solution chambers and API or API/cocrystal former (CCF) chambers in the fluid layer and pneumatic control lines and valves (1, 2) in the control layer. (c1−6) Schematics highlighting filling and mixing in 3 wells of the microfluidic crystallization platform. (c1) Empty platform; (c2) valve set 1 is actuated to start filling of the wells; (c3) microseed solution and PC or CCF solution is loaded into the crystallization wells; (c4) crystallization wells are completely filled, after which valve set 1 is closed; (c5) valve set 2 is opened and diffusional mixing between the adjacent chambers begins; (c6) valve set 2 is closed and diffusional mixing within the microseed and API or CCF chambers continues until equilibrium is reached.

seeds in subsequent crystallization trials to enhance crystal quality. This process is reiterated until diffraction quality crystals are formed. The process of consistently introducing microseeds in a crystallization trial is challenging, although robots to automate this process have been used with some success. Still, obtaining single and isolated diffraction quality crystals remains a challenge. An inexpensive, high throughput technology that can simplify the seeding protocol and enable good control over seed transfer would be instrumental in the crystallization and structure determination of solid forms of pharmaceuticals.

Progress in microfluidics has resulted in the development of microfluidic platforms for pharmaceutical crystallization of different solid forms, such as polymorphs, salts, and cocrystals.[13−20] Utilization of microfluidic platforms allows for solid form screening at earlier stages of drug development when only very small quantities of APIs are available. For example, platforms based on droplets,[17,19] patterned surfaces,[20] free interface diffusion,[14,16] antisolvent addition,[13] temperature control,[18] and evaporation[15] have been employed for pharmaceutical crystallization. Some of the aforementioned platforms allow for crystal harvesting and subsequent analysis via traditional approaches.[21−23] In contrast, some platforms have been reported that enable on-chip analysis of the solid forms, eliminating the need to manually harvest crystals.[14,15,24−26] For example, we have reported on microfluidic platforms for pharmaceutical solid form screening employing FID, antisolvent addition, and solvent evaporation that allow for subsequent solid form identification via on-chip Raman spectroscopy.[13−16] Similarly, microfluidic platforms comprised of X-ray transparent materials have been use for crystallization screening and X-ray data collection on-chip.[24−27]

Here, we report a microfluidic approach for pharmaceutical solid form screening that (1) enables crystallization optimization by crystal seeding and (2) allows for on-chip X-ray data collection from crystals formed, so the crystal structure of each

DOI: 10.1021/cg5016065
Cryst. Growth Des. 2015, 15, 1201−1209

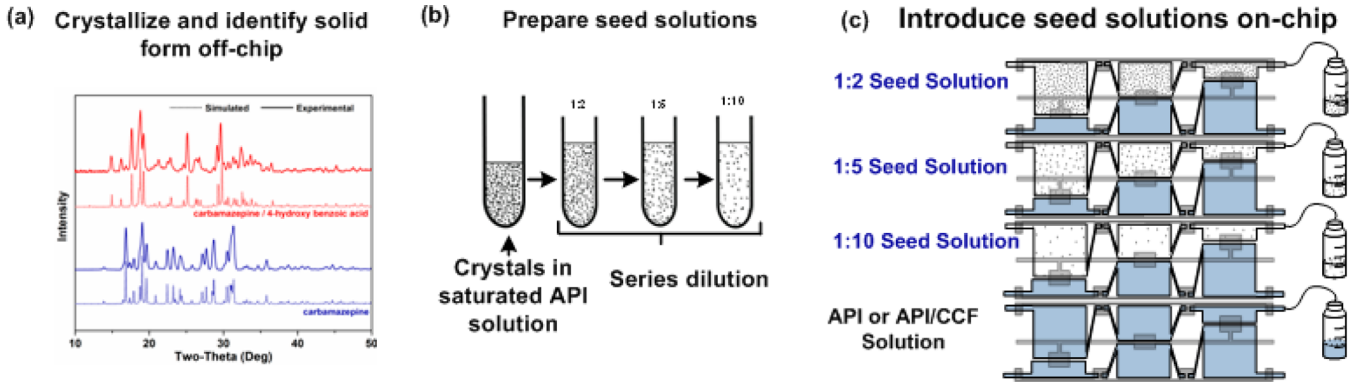

Figure 2. Protocol for setting up the on-chip seeding experiment. The API or the cocrystal is crystallized off-chip, and the solid form is verified via powder X-ray diffraction (a). The solid form crystals are crushed in a saturated API solution to prepare a seed solution (b). Then the seeding solutions are introduced on-chip along with API solution (or premixed API/CCF solutions) (c). Subsequently, the mixing valve is opened for 3 min to introduce seeds from the seed solution chamber to the API solution chamber (or API/CCF solution chamber).

solid form can be determined. We validate this microfluidic approach using model APIs (carbamazepine, piroxicam, and piracetam), as well as a cocrystal (carbamazepine/4-hydroxybenzoic acid). Due to small sample requirement of the crystallization optimization trials (about 5 μg/well), this microfluidic approach can be used in early stages of drug development.

2. EXPERIMENTAL SECTION

2.1. Chip Assembly. The crystallization platform (Figure 1) is comprised of thin polydimethylsiloxane (PDMS, General Electric RTV 615, Part A/B) fluid and control layers sandwiched between a cyclic olefin copolymer (COC, 6013 grade, TOPAS Advanced Polymers) support layer and a COC substrate layer. The platform is fabricated following the procedure previously reported[16] with a few modifications. Control layers (CL, 70 μm) and fluid layers (FL, 60 μm) were prepared by spin coating 5:1 A/B PDMS and 15:1 A/B PDMS at 1300 and 1550 rpm, respectively, onto silicon wafers (University wafer) patterned with a negative photoresist SU-8 2050 (MicroChem) and thermally cured on a hot plate (Dataplate 730 series, Barnstead Thermolyne). The COC-CL was assembled by irreversibly bonding a 2 mil (50 μm) COC sheet to the top of the control layer after treatment with oxygen plasma in plasma cleaner for 1 min (Harrick Plasma). Holes were drilled (Dremel 300 series drill) with a 750 μm (McMaster-Carr) drill bit to form inlets of the control lines in the COC-CL, and then the assembly was manually aligned on to the FL. The COC-CL-FL assembly was lifted off from the FL master and holes were drilled to form inlets and outlets in the FL. Next, a 3 mm thick PDMS block was irreversibly bonded to the top of the COC-CL-FL assembly, followed by punching of holes into the thick layer, resulting in the complete crystallization platform (Figure 1). See Supporting Information for more details on platform fabrication.

2.2. Chip Design and Fabrication. The 72-well microfluidic platform used here (Figure 1) is an adaptation of a design we reported previously.[13] Briefly, each of the 8 × 9 wells is comprised of a chamber for an API solution (or a premixed API/CCF solution) and an adjacent chamber for a microseed solution (Figure 1b). The dimensions of the chambers were varied to screen different volumetric ratios of the seed solutions and API solutions (or premixed API/CCF solutions). Each well has a height of 50 μm, a width of 1 mm, and a total length of 2 mm, resulting in well volumes of approximately 100 nL (combined volume of API solution or premixed API/CCF solution and microseed solution chambers, Figure 1). The "length" of the two compartments within the well are varied along each row of the microfluidic platforms such that the microseed to API solution (or microseed to API/CCF solution) ratios (L_{MS}-to-L_{API}) are 4:1, 3:1, 2:1, 1:1 (2×), 1:2, 1:3, and 1:4, as schematically shown in a 3 × 3 array in Figure 1b. Varying the relative size of the API or API/CCF solution and microseed solution chambers, as expressed in the length of the chambers (L_{MS} and L_{API}, Figure S2, Supporting Information), changes the concentration of seeds transferred from microseed chamber to API solution chamber (or premix API/CCF solution chamber). Another deviation compared with the previously reported design[13] is that the microchannels connecting adjacent chambers along each row of wells were designed to "zigzag" to reduce issues with dead volume and bubbles, ensuring faster and complete filling of large chambers (Figure 1). This microfluidic platform allows for 56 unique crystallization conditions to be tested in a single experiment. When ideal seeding conditions have been determined, the same microfluidic platforms are used to perform many replicates of the preferable condition.

2.3. Preparation of Active Pharmaceutical Ingredient and Cocrystal Former Solutions. To estimate the solubility of the API in the solvent, 50 mg of drug (carbamazepine, piroxicam, or piracetam) was dispensed into a 7 mL glass vial (Kimmble/Chase) and a solvent (acetonitrile, acetonitrile/methanol, or methanol) was pipetted into the glass vial in increments of 200 μL until the solid was completely dissolved. After each solvent addition, the mixture was vortexed (Maxi Mix II, Barnstead/Thermolyne) then allowed to sit for 5 min. Following this procedure, the solubility of carbamazepine, piroxicam, and piracetam were determined to be 37 mg/mL (0.16 M) in acetonitrile, 14.28 mg/mL (0.043 M) in an acetronitrile/methanol mixture (1:1 volume ratio), and 120 mg/mL (0.84 M) in methanol, respectively. Then, the solution was filtered, and the supernatant was used in crystallization experiments. The 4-hydroxybenzoic acid (cocrystal former) solution was prepared in an equimolar concentration (0.16 M) with the carbamazepine drug solution in acetonitrile.

2.4. Off-Chip Crystal Seed Preparation. To obtain seeds for on-chip seeding trails, the APIs and a cocrystal were crystallized off-chip. Seeds of carbamazepine were generated by dispensing 500 μL of 0.16 M carbamazepine in acetonitrile into a 1 mL glass vial. The vial was covered with Parafilm-M (American National Can Co. Chicago IL), and the solvent was allowed to evaporate through a small hole in the Parafilm (solvent evaporation rate of 6−24 μL/h). A similar procedure was used to generate seeds of piroxicam and piracetam in acetonitrile:methanol and methanol, respectively. To generate seeds of carbamazepine/4-hydroxybenzoic acid cocrystal, solutions of carbamazepine as described previously were mixed with equimolar 4-hydroxybenzoic acid solution in 1 mL glass vials. The mixture of solutions was vortexed then sealed by capping the glass vials to avoid solvent evaporation. After 2−5 h when no solid formation was observed, the cap from each glass vial was removed, and the glass vial was covered with Parafilm. A hole was made through the Parafilm to allow for slow solvent evaporation (in the range of 6−24 μL/h). The solvent was allowed to fully evaporate resulting in a deposition of crystals on the walls and bottom of the glass vial.

2.5. Powder X-ray Diffraction. To confirm the identity of the solid forms generated in the off-chip experiments, the powder X-ray diffraction patterns of the solids were collected and compared with the

DOI: 10.1021/cg5016065
Cryst. Growth Des. 2015, 15, 1201−1209

published data. Powder X-ray diffraction data was collected using a Bruker D8 Venture equipped with a four-circle κ diffractometer and Photon 100 detector. An IμS microfocus Cu source (λ = 1.54059 Å) supplied the multimirror monochromated incident beam. The sample was dispersed in a minimum amount of paratone oil and loaded onto a 0.3 mm loop and exposed for 180 s for several frames. The frames were merged and integrated from 5° to 60°. In the final spectrum, data was normalized to facilitate pattern matching, and the baseline was corrected using a Chebyshev polynomial.

2.6. Seed Solution Preparation. The procedure of preparing seed stock solutions and their off-chip dilutions is shown schematically in Figure 2. First, approximately 1.5 mg of the API or cocrystal crystals grown off-chip were harvested from the glass vial and carefully placed in the glass tube of a tissue homogenizer (Wheaton Tissue Grinder 2 mL with PTFE pestle), and 600 μL of saturated API solution was added to the glass vial, yielding a solution with an approximate seed concentration of 2.5 mg/mL. The crystals were then pulverized using the homogenizer, as reported previously,[28,29] until no crystal agglomerates could be seen in the glass tube using stereomicroscope (Leica MZ12.5) equipped with a digital camera (Leica DFC295) at about10× magnification. The resulting seed stock solution was then serially diluted with saturated drug solution with volumetric ratios of 1:2 (1.25 mg/mL), 1:5 (0.5 mg/mL), and 1:10 (0.25 mg/mL). Each successive dilution contains fewer and fewer seeds.

2.7. On-Chip Seeding Trial Setup. The diluted seed solutions (1:2, 1:5, and 1:10 dilutions) were introduced in alternating rows of the chip for crystallization experiments along with API solution (or API/CCF solution), as shown schematically in Figure 2. The last adjacent two rows served as the control experiment and only contain API solution (or API/CCF solution).

Reagents were introduced into the microfluidic chip using a vacuum pump coupled with a modified manifold with Teflon tubes and PDMS blocks to apply vacuum to the fluid routing inlets. Fluidic routing and mixing was controlled via an array of normally closed valves (two sets) incorporated in the control layer (Figure 1b).[13,30] The various solutions (API solution or premixed API/CCF solutions, seed solutions) were stored in microcentrifuge tubes (0.65 mL, VWR International) and connected to the microfluidic platform via tubing (PTFE #30 AWG, Cole-Parmer Instrument Company).) Valve set 1 (Figure 1c2) was actuated to introduce the API solution (or API/CCF solutions) and seed solutions in their respective wells, and vacuum suction was applied at the outlet of the row being filled. Valve set 1 was kept open for 1−2 min (Figure 1c2−c4) to ensure complete filling of the solutions in the wells and then closed to isolate the solutions in the wells. Next, valve set 2 was opened for about 3 min (Figure 1c5) to allow for mixing between the seed solution chamber and the premixed API solution (or API/CCF solution) chamber. Initially, when valve set 2 was actuated some convection due to displacement of the valve stop occurred, possibly transferring seeds between the microseed and API (or API/CCF) chambers. Valve set 2 was kept open for 5 min to allow diffusional mixing between the adjacent chambers. Next, valve set 2 was closed, and all tubing for pneumatic control and fluidic flow was disconnected (Figure 1c6). Diffusional mixing continued within the microseed API (or API/CCF) chamber after valve set 2 was closed, until equilibrium was reached in the chamber. The now completely filled chip was sealed with Crystal Clear Tape (Hampton Research HR4-511) and placed in a plastic Petri dish along with two microcentrifuge tubes filled with the solvent(s) used in the crystallization experiment to saturate the environment inside the Petri dish with solvent vapor. The Petri dish was sealed with Parafilm to further minimize loss of solvent vapor and was incubated at room temperature for 1 to 2 days. As solvent slowly evaporated from the sealed Petri dish, crystal growth was observed.

2.8. On-Chip Crystallization Monitoring. Throughout the incubation period, the wells were monitored for solid formation using an automated imaging setup comprised of an optical microscope (Leica Z16 APO) equipped with an autozoom lens (Leica 10447176), a digital camera (Leica DFC280), and a motorized $X-Y$ stage (Semprex KL66) controlled by Image Pro Plus 7.1 software (Media Cybernetics). Periodically, birefringent images of the wells were taken using crossed polarizers. The monitoring of the wells in the microfluidic platform was stopped once crystals were observed in multiple wells.

2.9. Unit Cell Determination of Single Crystals. The unit cell of good quality crystals was used to verify solid form and to identify crystallization conditions that yielded the desired solid form. To determine the unit cell, a diffraction quality single crystal was manually removed from the chip and mounted on a 0.3 mm loop using paratone oil. The sample was centered on the instrument and cryocooled to 100 K in a nitrogen supplied Oxford 700 Cryostream. Unit cell data was collected using a Bruker D8 Venture X-ray diffractometer equipped with a four-circle κ diffractometer and Photon 100 detector. A IμS microfocus Mo source (λ = 0.7107 Å) supplied the multimirror monochromated incident beam. Two series of ω scans consisting of 12 frames each were collected with an exposure time of 10 s. Diffraction spots with an $I/\sigma > 5$ were harvested from these 24 frames and indexed to determine the unit cell. The initial unit cell parameters were refined and assigned as one of the 14 Bravais lattice types. These values were compared with reported crystal structures for solid form verification.

2.10. On-Chip Single Crystal X-ray Data Collection. Prior to mounting the microfluidic platform, the platform was cut to fit on the goniometer. For data collection on the LS-CAT 21-ID-D and IMCA-CAT 17 ID-B beamline at Argonne National Lab, a 1 mm × 1.7 mm and 1.2 mm × 3 mm section of crystallization wells was cut from the platform, respectively. The resized pieces of the microfluidic platform were mounted on a standard magnetic goniometer mount (Hampton Research) with an attached metal tube. A slit cut into the metal tubing and a set-screw was used to secure samples, as reported previously.[24] Diffraction data was collected at room temperature. The sample-to-detector distance was varied depending on crystal quality (shorter distance for higher quality crystals). Data was collected using 1° steps with a 1 s exposure at an X-ray energy of 18 keV (λ = 0.689 Å, LS-CAT 21-ID-D) and of 17 keV (λ = 0.729 Å, IMCA-CAT 17 ID-B). Data from multiple crystals in the microfluidic platforms was collected over a range of 10°−40° (−5° to +5° or −20° to 20°) and an optimal subset of the frames was subsequently merged to obtain a complete data set.

The employment of thin layers of PDMS and X-ray transparent COC maximizes transmission of X-rays through the chip materials,[24] thereby enabling collection of high quality X-ray data from crystals formed on-chip. The characteristic scattering pattern of PDMS and COC observed in diffraction data collected on-chip occurs at relatively low angles of q-spacing or areas of low resolution diffraction (rings at 5.2 Å for COC and at 7.5 Å for PDMS) and does not affect the data collected at higher resolution. More details on the X-ray transparency of the chips studied here is provided in the Supporting Information (Figure 3S).

2.11. Analysis of X-ray Data Collected On-Chip. Analysis of X-ray diffraction data collected at the synchrotron source at Argonne was performed using HKL2000 software for indexing, refinement, integration, and scaling (HKL Research). The resolution range of the data was established based on the resolution shell at which I/σ fell above 2.0. Subsequent processing of crystallography data sets was done using several programs including WinGx, Shelx, Shelxe, Shelxl, and Shelxs to identify the space group, generate the electron density maps, and generate the final crystal structure images.

3. RESULTS AND DISCUSSION

3.1. Results of On-Chip Seeding Experiments. To validate the on-chip seeding approach four systems were studied: (i) carbamazepine/4-hydroxybenzoic acid, (ii) carbamazepine, (iii) piroxicam, and (iv) piracetam. The cocrystal of carbamazepine/4-hydroxybenzoic acid is known to have three polymorphic forms, designated as forms A−C.[31] Two of the polymorphs are made up of a 1:1 ratio of carbamazepine/4-hydroxybenzoic acid (form A and form C), and the third polymorph is composed of a different ratio (1:X) of

DOI: 10.1021/cg5016065
Cryst. Growth Des. 2015, 15, 1201−1209

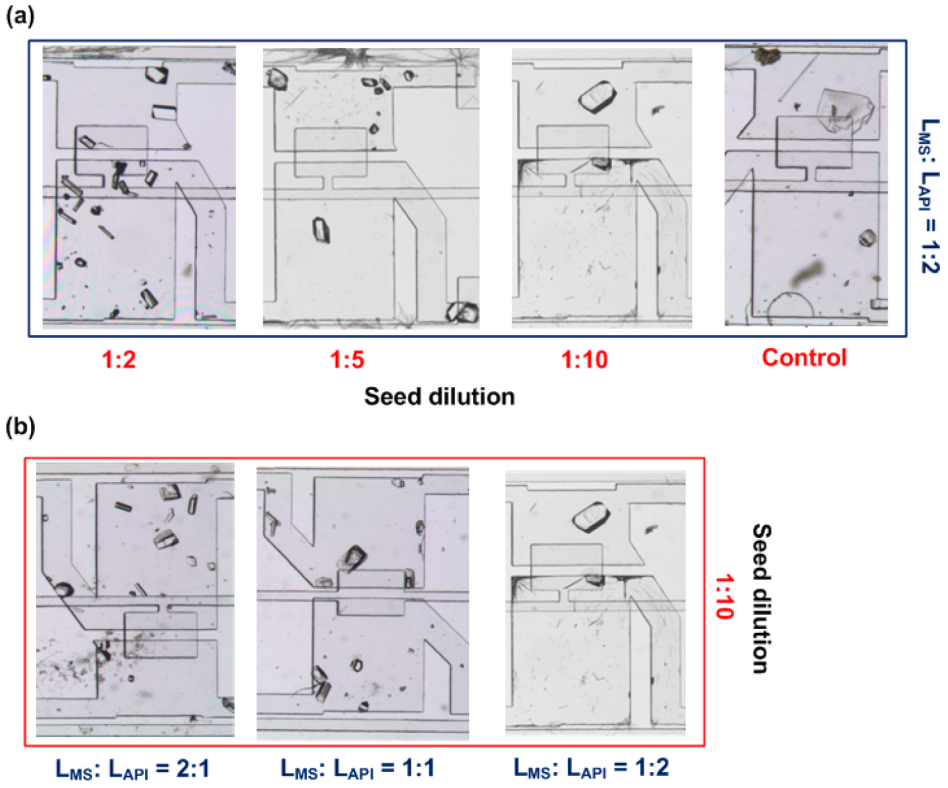

Figure 3. Results of the on-chip seeding experiment for carbamazepine/4-hydroxybenzoic acid cocrystal. The variation in the number and size of crystals can be observed as a function of (a) seed dilution ratio (in red) and (b) microseed to API solution (or premixed API/CCF solution) chamber ratio (L_{MS}/L_{API}, in blue). Off-chip and on-chip seed dilution helped to grow fewer isolated crystals.

carbamazepine/4-hydroxybenzoic acid (form B).[31] Form A is the most stable polymorphic form, with form C being metastable relative to form A at room temperature. In on-chip seeding experiments for carbamazepine/4-hydroxybenzoic acid cocrystal (Figure 3), we observed fewer and larger crystals upon increasing the dilution ratio from 1:2 to 1:10. This was expected since crystallization is primarily controlled by crystal growth of the cocrystals seeds. Similarly, when fewer cocrystal seeds were present (at higher dilution ratio), we saw a higher number of high quality crystals, Figure 4a. Polymorph form A was predominantly observed when microseeds of the same polymorph were used in these experiments. The seeds were confirmed to be form A by comparing experimental powder X-ray diffraction with simulated powder patterns from the known crystal structures. These results imply that seeding not only aids in growing single, isolated crystals but also aids crystallization of one particular polymorph or form of the cocrystal. We observed that seeding drastically increased the number of crystals compared with the control (Figure 4a), and we also observed that variation in the well geometry (L_{MS}/L_{API}) helped to control the number and size of crystals generated. When the L_{MS}/L_{API} is varied from 1:2 to 2:1, the size of the resulting crystals decreased while the number of crystals increased for all dilution ratios (Figure 3b).

Carbamazepine is known to have four polymorphic forms designated as forms I–IV.[32] The most stable polymorph is form III; however, the difference in energy from the most stable to the least stable polymorph is less than 0.7 kcal/mol.[31] The seeds used in our experiment were found to be polymorph form III. From our experimental results, we found that the control wells resulted in a mixture of form II (needles) and small form III (prisms),[33] Figure 4b, and employment of the

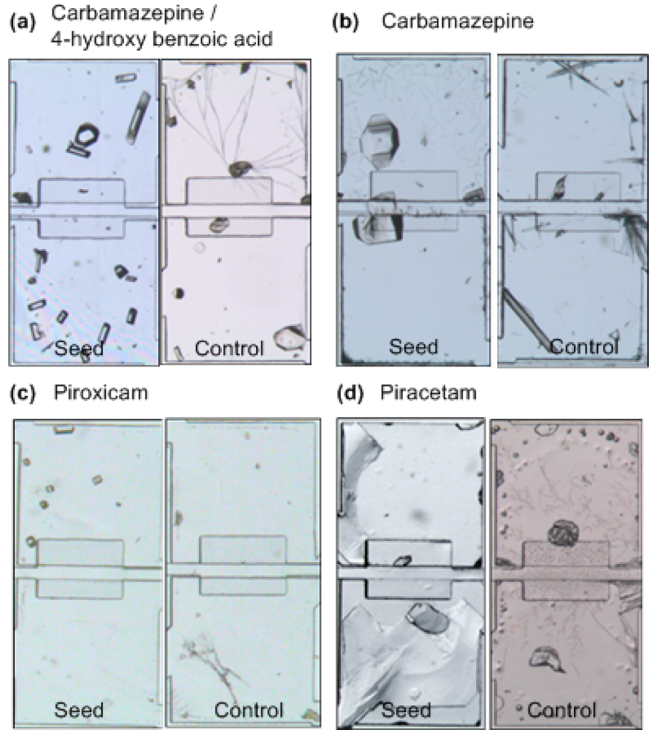

Figure 4. Comparison of crystallization results with (seed) and without seeding (control). All images are of a 1:1 microseed to API solution (or premixed API/CCF solution) chamber ratio. Dilution ratios for the images are as follows: (a) 1:2, (b) 1:5, (c) 1:5, and (d) 1:2.

DOI: 10.1021/cg5016065
Cryst. Growth Des. 2015, 15, 1201–1209

seeding method directed the crystallization toward predominant formation of form III crystals. In the control experiment, unit cell analysis of diffraction quality crystals was used to distinguish between crystal forms. Due to the presence of multiple solid forms, no on-chip diffraction data was collected from the control wells.

Piroxicam was the third compound studied, and piroxicam has three known polymorphs. Although the notation used to describe the polymorphs of piroxicam varies by publications, we will denote the polymorphs as forms I–III.[34] Form I is the most stable polymorph, and the energy difference between form I and form II was calculated to be approximately 1.23 kcal/mol.[34] Our experimental results showed that in the case of piroxicam, the control experiment yielded clusters of very thin needles (form II), whereas the seeding experiments, seeds confirmed as form I, yielded well-formed rectangular prisms (form I), Figure 4c.[34] In the case of piroxicam, the use of microseed dilution did not have a significant effect on crystal number or size as seen with carbamazepine/4-hydroxybenzoic acid, but diffraction quality crystals were observed in all conditions when seeds were employed.

Piracetam was the final compound studied, and piracetam has five known polymorphs, denoted as forms I–V. For piracetam, the control experiment yielded a gel, and the 1:5 and 1:10 microseed dilution experiments yielded large but poorly formed and twinned crystals. The 1:2 microseed dilution experiment on-chip consistently yielded very large diffraction quality crystals. We believe that the crystal growth rate of piracetam may be too low, and nucleation occurred at all conditions due to solvent loss. At lower dilution ratios, more seeds were present so increased supersaturation led to crystal growth while keeping the supersaturation level low enough to prevent nucleation. The ease of experimental setup and utilization of small quantities of API allows for screening many seeding conditions. Images of carbamazepine/4-hydroxybenzoic acid, carbamazepine, piroxicam, and piracetam crystals grown with the seeding approach are compared with control experiments in Figure 4. We show that seeding on-chip can lead to more reproducible diffraction crystal quality crystals. In some cases, the control experiment did yield diffraction quality crystals, but the results were not consistent across experimental trials.

3.2. On-Chip X-ray Data Collection. Once crystals were formed on-chip, X-ray data was collected on crystals while they still resided within the microfluidic wells. In traditional crystallography, crystals are manually looped out, cryo-cooled, mounted in a cryo-stream, and rotated in the X-ray beam for collection of multiple data wedges. To collect X-ray data on crystals residing within the microfluidic platform, we adopted a strategy reported in our previous work for data collection on protein crystals.[24] First we reduced the size of the microfluidic platform by cutting out a few rows or columns of wells as described in the Experimental Section (On-chip Single Crystal X-ray Data Collection), and then we mounted this section of the chip in the beamline described in the Supporting Information, Figure S4. The chip was still too large to fit within typical cryo-streams on crystallography beamlines, so data was collected at room temperature. An advantage of single crystal X-ray data collection at room temperature is a better fit between calculated and experimentally collected powder X-ray diffraction patterns. The geometry of the microfluidic platform makes complete rotation of the chip (−180° to 180°) for complete data set collection challenging. Instead, we collected small wedges of data (10°–40° per crystal) from a large number of crystals and later merged these frames to form a complete data set. A flow sheet outlining data collection and structure determination is provided in the Supporting Information, Figure S5. This approach works provided the orientation of the crystals grown is mostly random. Previously, this method of merging data sets from multiple crystals has been used successfully to obtain structural information from tiny or fragile crystals or crystals that suffer from excessive radiation damage.[35,36]

3.3. X-ray Data Analysis. The data in this study was collected at room temperature using the method described in the on-chip X-ray data collection section. The maximum resolution diffraction spots obtained from carbamazepine/4-hydroxybenzoic acid (Figure 5b) and carbamazepine was ~0.7

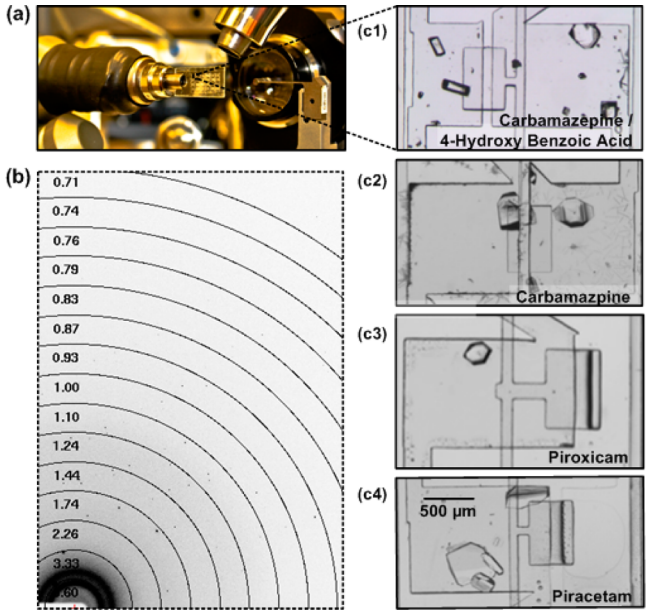

Figure 5. (a) The microfluidic chip mounted at the Argonne beamline (LS CAT 21-ID-D). (b) Example of diffraction data for the carbamazepine/4-hydroxybenzoic acid cocrystal. The background from the chip material can be observed in the form of dark rings at low resolutions. For this example, data was collected for the solid form at a resolution as high as 0.7 Å. (c1–4) Crystals of different compounds in individual wells: carbamazepine/4-hydroxybenzoic acid (c1), carbamazepine (c2), piroxicam (c3), and piracetam (c4).

Å, indicative of the high quality of the crystals obtained on-chip as a result of seeding. The final structure for all the molecules: carbamazepine/4-hydroxybenzoic acid (Figure 6a), carbamazepine (Figure 6b), piroxicam (Figure 6c), and piracetam (Figure 6d) was solved to a 0.7 Å resolution with 99.7%, 89.4%, 96.3%, and 86.8% completeness, respectively.

Table 1 provides important crystallographic information about the different solid forms crystallized on-chip. A comparison of the important crystallographic data between the microfluidic approach and the traditional approach is provided in the Supporting Information (Table S1). Compared with the previously reported structures for carbamazepine/4-hydroxybenzoic acid, carbamazepine, piroxicam, and piracetam (CSD codes: MOXIF, CBMZPN01, BIYSEH, and BISMEV01, respectively), the carbamazepine/4-hydroxybenzoic acid and carbamazepine structures were solved at a similar resolution

DOI: 10.1021/cg5016065
Cryst. Growth Des. 2015, 15, 1201–1209

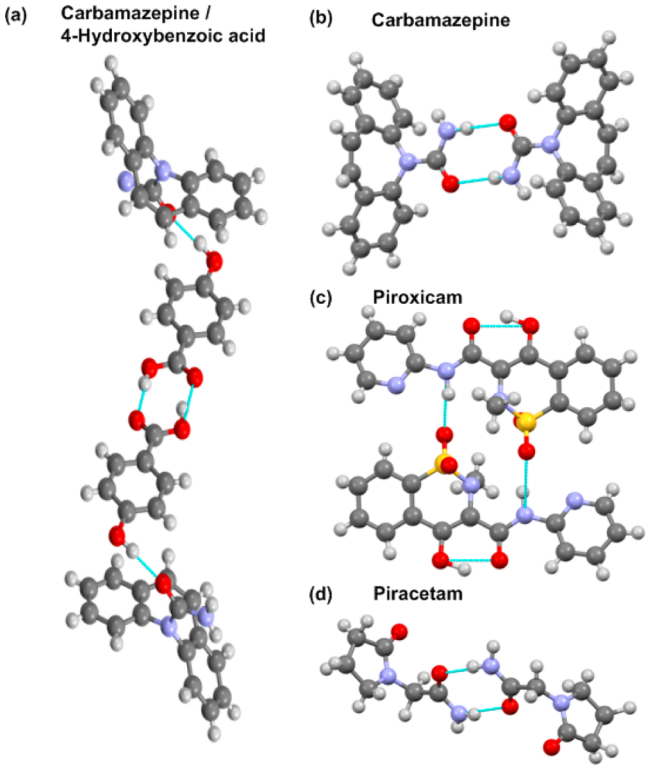

Figure 6. Solved structures for (a) carbamazepine/4-hydroxybenzoic acid cocrystal, (b) carbamazepine, (c) piroxicam, and (d) piracetam.

using the microfluidic approach reported. More data is needed for piroxicam and piracetam for better structure resolution.

3.4. Summary of Results. The microfluidic platform developed for crystallization optimization provides a simplified crystal seeding method for growth of crystals with good diffraction quality. Use of pneumatic valves allows precise metering of small solution volumes with ease. The design of the platform with varying volumetric ratios of microseed solution and API solution (or API/CCF solution) allows a wide range of crystallization conditions to be screened without extensive manual experimental setup (solution preparation and pipetting). In addition to simple experimental setup, the microfluidic platform provides greater control over solution mixing and solvent evaporation. Diffusional mixing between seed solution and API solution (or API/CCF solution) allows the concentrations within each chamber to gradually change, enhancing the chances of the supersaturation level maintaining the crystal growth zone instead of traversing into crystal nucleation zone. By incubating the platforms in a solvent vapor atmosphere, the rate of solvent evaporation is further reduced leading to better crystal growth.

A key advantage of this microfluidic platform is the compatibility with solid form characterization methods (optical microscopy, Raman, and X-ray diffraction) eliminating the time-consuming task of crystal harvesting followed by off-chip analysis of each crystal individually. In an on-chip experiment, identification of crystalline solids and diffraction quality crystals with optical microscopy is relatively straightforward. With off-chip experiments, identification of single diffraction quality crystals among many poorly formed crystals can be challenging. In addition, thin crystals, often too fragile to be harvested, can be analyzed on-chip.

Comparing the results of off-chip seeding experiments (in 1 mL glass vials) for carbamazepine and carbamazepine/4-hydroxybenzoic acid with those of on-chip seeding revealed that the outcomes of on-chip experiments typically are better in terms of the quality of the crystals obtained, the ease by which they can be found within a well, and the number of experiments leading to crystals. These better outcomes of on-chip experiments are the result of better control over solvent

Table 1. Results of on-Chip X-ray Diffraction Data Analysis

	carbamazepine/4-hydroxybenzoic acid	carbamazepine	piroxicam	piracetam
empirical formula	$C_{22}H_{18}N_2O_4$	$C_{15}H_{12}N_2O$	$C_{15}H_{13}N_3O_4S$	$C_6H_{10}N_2O_2$
formula weight	374.38	236.27	331.348	142.16
temperature (K)	298	298	298	298
wavelength (Å)	0.68875	0.68875	0.72932	0.72932
cryst syst	monoclinic	monoclinic	monoclinic	monoclinic
space group	P $2_1/c$	P $2_1/n$	P $2_1/c$	P $2_1/n$
a (Å)	7.112	7.542	7.135	6.505
b (Å)	12.764	11.155	15.150	6.418
c (Å)	20.288	13.919	13.955	16.423
α (deg)	90	90	90	90
β (deg)	92.143	92.885	97.408	92.170
γ (deg)	90	90	90	90
vol (Å^3)	1840.410	1169.500	1495.880	685.2
Z	4	4	4	4
density (calcd) (mg/m^3)	1.351	1.342	1.471	1.378
absorp coeff (mm^{-1})	0.089	0.081	0.300	0.128
θ range for data collection (deg)	0.973−28.200	2.620−26.59	3.430−29.082	3.216−27.103
completeness to θ	98.8	89.800	96.3	86.8
reflns collected	5124	2538	3579	1324
indep reflns	4400	2252	1554	684
GOF of F^2	0.983	1.077	0.796	0.978
final R indices [$I > 2\sigma(I)$]	R_1 = 0.0540, wR_2 = 0.1512	R_1 = 0.0395, wR_2 = 0.1119	R_1 =0 0.1462, wR_2 = 0.2483	R_1 = 0.1091, wR_2 = 0.1507
R indices (all data)	R_1 = 0.0586, wR_2 =0.1604	R_1 = 0.430, wR_2 = 0.1167	R_1 = 0.1506, wR_2 = 0.2522	R_1 = 0.1150, wR_2 = 0.1602

DOI: 10.1021/cg5016065
Cryst. Growth Des. 2015, 15, 1201−1209

evaporation and the addition of seeds (often too many seeds are added in an off-chip experiments, leading to showers of crystals), as well as better control over mixing of the seed solution with the API solution.

4. CONCLUSIONS

In this paper, we reported on a microfluidic approach to optimize crystallization and subsequently determine structures of pharmaceutical solid forms via on-chip X-ray analysis. Specifically, we successfully employed a 72-well (8 × 9) array-based microfluidic platform to screen unique seeding conditions of three model APIs (piroxicam, piracetam, and carbamazepine) and a cocrystal (carbamazepine/4-hydroxybenzoic acid) by varying the volumetric ratio from 1:4 to 4:1 of API solution (or API/CCF solution) and microseed solution. Screening microseed dilutions along rows helped determine optimized conditions for crystallization of solid forms of pharmaceuticals. In the case of carbamazepine, this seeding approach also aided in producing crystals of a specific solid form (form II) over a mixture of forms II and III. The platform was engineered to enable X-ray data collection on-chip by minimizing material thickness, which maximizes the transmission of X-rays. Data was collected on different crystals and later merged together to form a complete data set and resulted in the determination of the structure of pharmaceutical solid forms. Key attractive features of these platforms are easy handling and simplified seeding while using small quantities of PC (about 5 μg/well), and X-ray analysis. Ease of operation, requiring only a vacuum source, enables immediate application of these chips in laboratories for solid form crystallization.

Going forward, better control over crystallization outcomes would be expected if temperature control was integrated with the microfluidic platforms. A wider range of supersaturation conditions could be screened and experiments could be conducted in the metastable zone (growth zone) to maximize the advantages of seeding. One can also foresee using this platform to study the effects of additives such as polymers, surfactants, and antisolvents on solid form crystallization, crystal morphology, and polymorphism of APIs as well as on stabilization of the amorphous forms of APIs.

■ ASSOCIATED CONTENT

Supporting Information

Description of different levels of supersaturation in crystallization of small molecules, detailed information about fabrication of the platforms, optical micrograph of 72-well microfluidic platform filled with food dyes, explanation of X-ray transparency of the microfluidic platform, optical micrograph of the setup of the microfluidic chip on the Argonne beamline for X-ray data collection, flow sheet demonstrating X-ray data collection and analysis procedure, and comparison of PXRD patterns for solid forms crystallized using our off-chip experiments to PXRD pattern for intended solid forms available in the literature. This material is available free of charge via the Internet at http://pubs.acs.org.

■ AUTHOR INFORMATION

Corresponding Authors

*Yuchuan Gong. Phone: (847) 938-6642. Fax: (847) 937-2417. E-mail: yuchuan.gong@abbvie.com.

*Paul J. A. Kenis. Phone: (217) 265-0523. Fax: (217) 333-5052. E-mail: kenis@illinois.edu. Web Address: http://www.scs.uiuc.edu/~pkgroup/.

Author Contributions

⊥These authors (E.M.H. and S.G.) contributed equally to this work. The University of Illinois at Urbana, Champaign and AbbVie jointly participated in study design, research, data collection, analysis and interpretation of data, writing, reviewing, and approving the publication. Elizabeth M. Horstman and Sachit Goyal are graduate students, Ashtamurthy Pawate is a research scientist, Garam Lee is an undergraduate student, and Paul J. A. Kenis is a professor at the University of Illinois at Urbana, Champaign.

Notes

The authors declare the following competing financial interest(s): Geoff G. Z. Zhang and Yuchuan Gong may own AbbVie stock.

■ ACKNOWLEDGMENTS

This material is based upon work supported by the National Science Foundation Graduate Research Fellowship Program under Grant Number DGE-1144245 (E.M.H.). We thank AbbVie Laboratories for financial support. Part of this work made use of the facilities in the Micro- & Nanotechnology Laboratory as well as the Frederick Seitz Materials Research Laboratory Central Facilities at University of Illinois at Urbana−Champaign, which is partially supported by the U.S. Department of Energy under Grants DE-FG02-07ER46453 and DE-FG02-07ER46471. We thank Dr. Russell Judge from AbbVie for arranging access to the 17 BM beamline at Argonne National Laboratory for X-ray data collection, and Dr. Kenton L. Longenecker and Dr. Rodger F. Henry from AbbVie for help with the initial analysis of the X-ray data collected at the 21-ID-D and 17 ID beamlines at Argonne National Laboratory. Use of the Advanced Photon Source (APS), Argonne National Laboratory, was supported by the US Department of Energy, Office of Basic Energy Sciences, under Contract No. DE-AC02-06CH11357, as well as UIUC. We thank Dr. Joseph Brunzelle, Dr. Keith Brister, and Dr. Spencer Anderson from LS-CAT (beamline 21-ID-D), as well as Dr. Lisa J. Keefe and Dr. Anne Mulichak from IMCA-CAT, at APS for help in data collection at the 21-ID-D and 17-BM beamlines, respectively. We also thank Dr. Danielle Gray and Dr. Jeffery Bertke for help with X-ray experiments at the University of Illinois, collection and analysis of the powder X-ray data on the crystals grown in off-chip experiments, and determination of unit cells of the crystals grown inside the microfluidic platforms. We thank Eric Hansohl Kim for help in creating figures. We thank Jose Gallegos-Lopez for help in the fabrication and design of microfluidic platforms.

■ REFERENCES

(1) Gardner, C. R.; Almarsson, O.; Chen, H. M.; Morissette, S.; Peterson, M.; Zhang, Z.; Wang, S.; Lemmo, A.; Gonzalez-Zugasti, J.; Monagle, J.; Marchionna, J.; Ellis, S.; McNulty, C.; Johnson, A.; Levinson, D.; Cima, M. Application of high throughput technologies to drug substance and drug product development. *Comput. Chem. Eng.* **2004**, *28*, 943−953.

(2) Morissette, S. L.; Almarsson, O.; Peterson, M. L.; Remenar, J. F.; Read, M. J.; Lemmo, A. V.; Ellis, S.; Cima, M. J.; Gardner, C. R. High-throughput crystallization: Polymorphs, salts, co-crystals and solvates of pharmaceutical solids. *Adv. Drug Delivery Rev.* **2004**, *56*, 275−300.

(3) Almarsson, O.; Hickey, M. B.; Peterson, M. L.; Morissette, S. L.; Soukasene, S.; McNulty, C.; Tawa, M.; MacPhee, J. M.; Remenar, J. F. High-throughput surveys of crystal form diversity of highly polymorphic pharmaceutical compounds. *Cryst. Growth Des.* **2003**, *3*, 927−933.

DOI: 10.1021/cg5016065
Cryst. Growth Des. 2015, 15, 1201−1209

(4) Jorgensen, W. L.; Duffy, E. M. Prediction of drug solubility from structure. *Adv. Drug Delivery Rev.* **2002**, *54*, 355−66.
(5) Tung, H.-H. Industrial Perspectives of Pharmaceutical Crystallization. *Org. Process Res. Dev.* **2012**, *17*, 445−454.
(6) Bergfors, T. Seeds to crystals. *J. Struct. Biol.* **2003**, *142*, 66−76.
(7) Khurshid, S.; Haire, L. F.; Chayen, N. E. Automated seeding for the optimization of crystal quality. *J. Appl. Crystallogr.* **2010**, *43*, 752−756.
(8) Nagy, Z. K.; Braatz, R. D. Advances and new directions in crystallization control. *Annu. Rev. Chem. Biomol. Eng.* **2012**, *3*, 55−75.
(9) Braatz, R. D. Advanced control of crystallization processes. *Annu. Rev. Control* **2002**, *26*, 87−99.
(10) Goh, L.; Chen, K.; Bhamidi, V.; He, G.; Kee, N. C.; Kenis, P. J.; Zukoski, C. F., 3rd; Braatz, R. D. A Stochastic Model for Nucleation Kinetics Determination in Droplet-Based Microfluidic Systems. *Cryst. Growth Des.* **2010**, *10*, 2515−2521.
(11) Chayen, N. E.; Saridakis, E. Protein crystallization: from purified protein to diffraction-quality crystal. *Nat. Methods* **2008**, *5*, 147−153.
(12) Beckmann, W.; Otto, W.; Budde, U. Crystallisation of the Stable Polymorph of Hydroxytriendione: Seeding Process and Effects of Purity. *Org. Process Res. Dev.* **2001**, *5*, 387−392.
(13) Thorson, M. R.; Goyal, S.; Gong, Y. C.; Zhang, G. G. Z.; Kenis, P. J. A. Microfluidic approach to polymorph screening through antisolvent crystallization. *CrystEngComm* **2012**, *14*, 2404−2412.
(14) Thorson, M. R.; Goyal, S.; Schudel, B. R.; Zukoski, C. F.; Zhang, G. G.; Gong, Y.; Kenis, P. J. A microfluidic platform for pharmaceutical salt screening. *Lab Chip* **2011**, *11*, 3829−3837.
(15) Goyal, S.; Thorson, M. R.; Schneider, C. L.; Zhang, G. G.; Gong, Y.; Kenis, P. J. A microfluidic platform for evaporation-based salt screening of pharmaceutical parent compounds. *Lab Chip* **2013**, *13*, 1708−1723.
(16) Goyal, S.; Thorson, M. R.; Zhang, G. G. Z.; Gong, Y. C.; Kenis, P. J. A. Microfluidic Approach to Cocrystal Screening of Pharmaceutical Parent Compounds. *Cryst. Growth Des.* **2012**, *12*, 6023−6034.
(17) Laval, P.; Crombez, A.; Salmon, J.-B. Microfluidic Droplet Method for Nucleation Kinetics Measurements. *Langmuir* **2009**, *25*, 1836−1841.
(18) Laval, P.; Lisai, N.; Salmon, J. B.; Joanicot, M. A microfluidic device based on droplet storage for screening solubility diagrams. *Lab Chip* **2007**, *7*, 829−834.
(19) Ildefonso, M.; Revalor, E.; Punniam, P.; Salmon, J. B.; Candoni, N.; Veesler, S. Nucleation and polymorphism explored via an easy-to-use microfluidic tool. *J. Cryst. Growth* **2012**, *342*, 9−12.
(20) Lee, A. Y.; Lee, I. S.; Dette, S. S.; Boerner, J.; Myerson, A. S. Crystallization on confined engineered surfaces: a method to control crystal size and generate different polymorphs. *J. Am. Chem. Soc.* **2005**, *127*, 14982−14983.
(21) Hansen, C. L.; Skordalakes, E.; Berger, J. M.; Quake, S. R. A robust and scalable microfluidic metering method that allows protein crystal growth by free interface diffusion. *Proc. Natl. Acad. Sci. U. S. A.* **2002**, *99*, 16531−16536.
(22) Zheng, B.; Roach, L. S.; Ismagilov, R. F. Screening of protein crystallization conditions on a microfluidic chip using nanoliter-size droplets. *J. Am. Chem. Soc.* **2003**, *125*, 11170−11171.
(23) Perry, S. L.; Roberts, G. W.; Tice, J. D.; Gennis, R. B.; Kenis, P. J. Microfluidic Generation of Lipidic Mesophases for Membrane Protein Crystallization. *Cryst. Growth Des.* **2009**, *9*, 2566−2569.
(24) Guha, S.; Perry, S. L.; Pawate, A. S.; Kenis, P. J. Fabrication of X-ray compatible microfluidic platforms for protein crystallization. *Sens. Actuators, B* **2012**, *174*, 1−9.
(25) Dhouib, K.; Khan Malek, C.; Pfleging, W.; Gauthier-Manuel, B.; Duffait, R.; Thuillier, G.; Ferrigno, R.; Jacquamet, L.; Ohana, J.; Ferrer, J. L.; Theobald-Dietrich, A.; Giege, R.; Lorber, B.; Sauter, C. Microfluidic chips for the crystallization of biomacromolecules by counter-diffusion and on-chip crystal X-ray analysis. *Lab Chip* **2009**, *9*, 1412−1421.
(26) Ng, J. D.; Clark, P. J.; Stevens, R. C.; Kuhn, P. In situ X-ray analysis of protein crystals in low-birefringent and X-ray transmissive plastic microchannels. *Acta Crystallogr., Sect. D: Biol. Crystallogr.* **2008**, *D64*, 189−197.
(27) Kisselman, G.; Qiu, W.; Romanov, V.; Thompson, C. M.; Lam, R.; Battaile, K. P.; Pai, E. F.; Chirgadze, N. Y. X-CHIP: An integrated platform for high-throughput protein crystallization and on-the-chip X-ray diffraction data collection. *Acta Crystallogr., Sect. D: Biol. Crystallogr.* **2011**, *D67*, 533−539.
(28) Luft, J. R.; DeTitta, G. T. A method to produce microseed stock for use in the crystallization of biological macromolecules. *Acta Crystallogr., Sect. D: Biol. Crystallogr.* **1999**, *D55*, 988−993.
(29) McPherson, A. *Introduction to Macromolecular Crystallography*; Wiley-Blackwell: Hoboken, NJ, 2009; Vol. *63*.
(30) Schudel, B. R.; Choi, C. J.; Cunningham, B. T.; Kenis, P. J. Microfluidic chip for combinatorial mixing and screening of assays. *Lab Chip* **2009**, *9*, 1676−1680.
(31) Childs, S. L.; Wood, P. A.; Rodriguez-Hornedo, N.; Reddy, L. S.; Hardcastle, K. I. Analysis of 50 Crystal Structures Containing Carbamazepine Using the Materials Module of Mercury CSD. *Cryst. Growth Des.* **2009**, *9*, 1869−1888.
(32) Grzesiak, A. L.; Lang, M.; Kim, K.; Matzger, A. J. Comparison of the four anhydrous polymorphs of carbamazepine and the crystal structure of form I. *J. Pharm. Sci.* **2003**, *92*, 2260−2271.
(33) Reboul, J. P.; Cristau, B.; Soyfer, J. C.; Astier, J. P. 5H-Dibenz[b,f]azépinecarboxamide-5 (carbamazépine). *Acta Crystallogr., Sect. B: Struct. Crystallogr. Cryst. Chem.* **1981**, *B37*, 1844−1848.
(34) Sheth, A. R.; Bates, S.; Muller, F. X.; Grant, D. J. W. Polymorphism in piroxicam. *Cryst. Growth Des.* **2004**, *4*, 1091−1098.
(35) Jaakola, V. P.; Griffith, M. T.; Hanson, M. A.; Cherezov, V.; Chien, E. Y. T.; Lane, J. R.; IJzerman, A. P.; Stevens, R. C. The 2.6 Angstrom Crystal Structure of a Human A(2A) Adenosine Receptor Bound to an Antagonist. *Science* **2008**, *322*, 1211−1217.
(36) Cherezov, V.; Rosenbaum, D. M.; Hanson, M. A.; Rasmussen, S. G. F.; Thian, F. S.; Kobilka, T. S.; Choi, H. J.; Kuhn, P.; Weis, W. I.; Kobilka, B. K.; Stevens, R. C. High-resolution crystal structure of an engineered human beta(2)-adrenergic G protein-coupled receptor. *Science* **2007**, *318*, 1258−1265.

DOI: 10.1021/cg5016065
Cryst. Growth Des. 2015, 15, 1201−1209